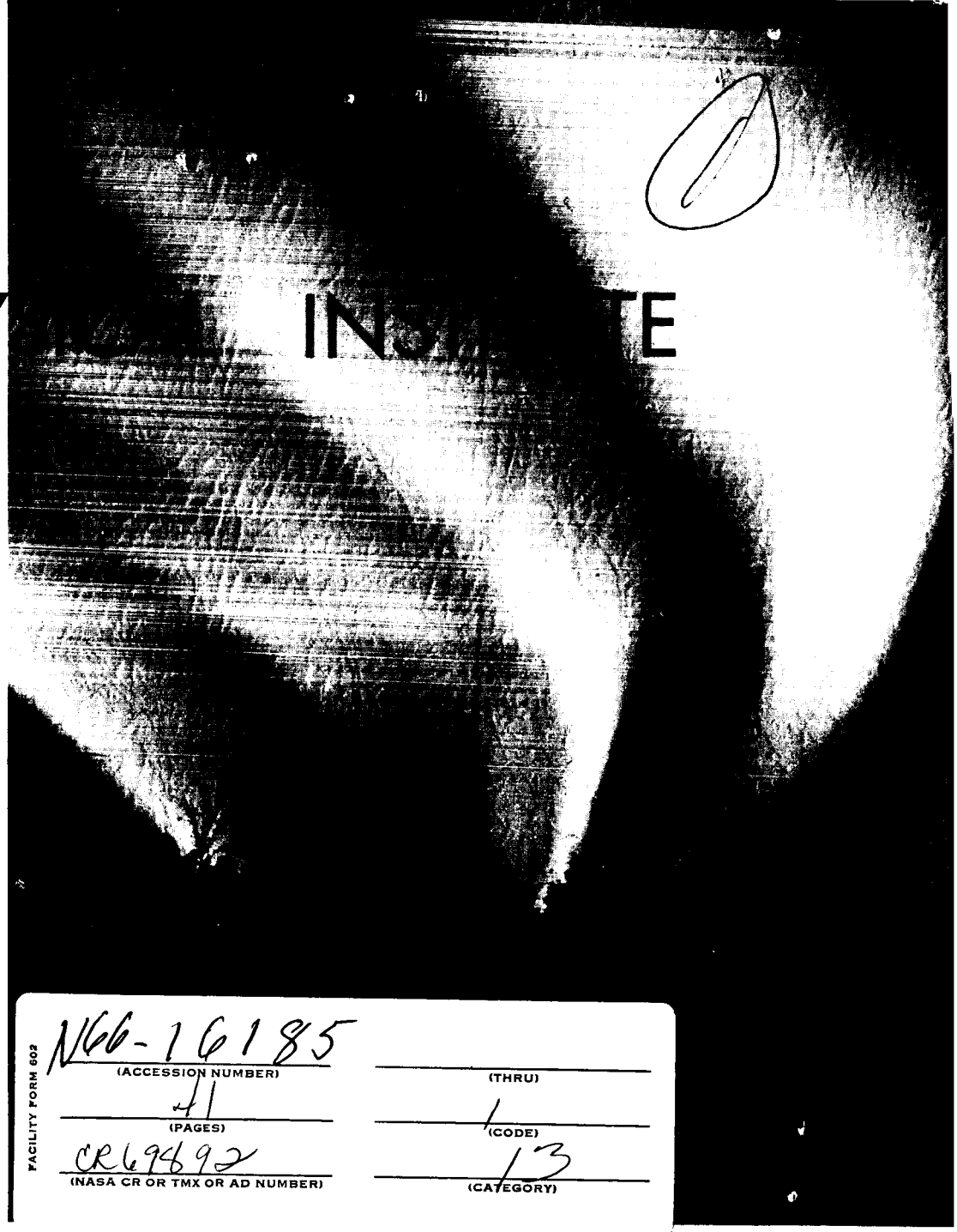

# GEOPHY[illegible] IN[illegible]TE


**UNIVERSITY OF ALASKA**

**COLLEGE, ALASKA**
**UAG R-171**




## EFFECTIVE RECOMBINATION COEFFICIENT IN D-REGION

by


**R. Parthasarathy and D. B. Rai**





**September 1965**
**SCIENTIFIC REPORT NO. 1**
**Grant NAS5-3595**

**of the**

**NATIONAL AERONAUTICS AND SPACE ADMINISTRATION**
**Washington, D. C.**

GEOPHYSICAL INSTITUTE

of the

UNIVERSITY OF ALASKA

Scientific Report No. 1

# EFFECTIVE RECOMBINATION COEFFICIENT IN D-REGION

by

R. Parthasarathy and D. B. Rai

NASA Grant No. NAS-5-3595

September 1965

Principal Investigator:

R. Parthasarathy

Approved by:

K. B. Mather

Keith B. Mather
Director

# EFFECTIVE RECOMBINATION COEFFICIENT IN D-REGION

R. Parthasarathy and D. B. Rai

Geophysical Institute
University of Alaska
College, Alaska

## ABSTRACT

16 185

The effect of the meteoric dust particles on the steady state distribution of electrons and ions in the lower ionosphere (50 - 90 km) has been investigated. It is shown that the effective recombination coefficient obtained is higher than that obtained by ignoring the presence of dust. The expression for the effective recombination coefficient thus obtained is of the form

$$\alpha_{eff} = (\alpha_d + \lambda\alpha_i)(\eta + \gamma\lambda) + \frac{D_e + \lambda D^-}{N_e}$$

where $D_e$, $D^+$ and $D^-$ are the dust capture coefficients for electrons, positive ions and negative ions respectively; $\eta$ and $\gamma$ are the ratios $D_e/D^+$ and $D^-/D^+$ respectively. The other symbols have the usual meanings. In the limit of zero dust concentration this expression reduces to the one derived by ignoring dust, i.e.

$$\alpha_{eff} = (1 + \lambda)(\alpha_d + \lambda\alpha_i)$$

The coefficients $D_e$, $D^+$ and $D^-$ are derived by an extension of Natanson's theory of charging of aerosols by capture of ions. The height dependence of these coefficients comes mainly through the height distribution of the dust particles, for which Divari's results from twilight studies are utilized. It

over

is found that only particles with radius of the order of tenth of a micron or larger contribute significantly. The recombination coefficients for the region 50 - 90 km have thus been computed and are in agreement with those deduced empirically by us from the multiple frequency (5 - 50 Mc/s) radiowave absorption data in the auroral zone. The empirical method consisted of comparing the electron density profile derived from the multiple frequency radiowave absorption with the ionization rate profile calculated using satellite-measured particle flux.

Author

## 1. Introduction

During the past few years, there has been a considerable amount of work dealing with the many physical processes that determine the steady state distribution of electrons and positive and negative ions in the lower regions of the ionosphere. Even though the processes involved are rather complex it has been possible to obtain some reasonable estimates of the rates of these processes, from which one can assemble an "effective recombination coefficient". Taking into consideration the most important known processes in the region, Webber (1962) has deduced the "effective recombination coefficient" for different altitudes. They are substantially lower than the values inferred earlier, for example, by Bailey (1959) and Mitra (1959), or those more recently inferred from ionospheric observations by other workers (Belrose et al, 1964; Whitten et al, 1965; McDiarmid et al, 1964; Adams and Masley, 1965). The coefficients deduced by us from the multiple frequency radiowave absorption data are also higher, and it is highly improbable that these high values could be attributed in all the cases to the uncertainties in determining the effective recombination coefficient. This leads one to the view that some additional factor other than molecular processes, must be operative and be affecting the steady state distribution of the electrons and ions in the lower ionosphere.

A possible factor of this type might be the presence of dust particles. It is generally known that the dust particles present in an ionized gas considerably affects the electron-ion ratio (Dimick and Soo, 1964; Rosen, 1962), and one would thus expect the dust particles present in the D-region to play some role in the steady state distribution of the electrons and ions. The object of the present paper is two-fold: In section 2 of this paper, the effective recombination coefficient for different altitudes in the D-region is derived from the multiple frequency radiowave absorption data. In section 3,

an expression for the effective recombination coefficient is obtained, taking into account the presence of dust particles. The expression is shown to reduce to the usual form when the dust particle concentration is negligible. The rate of capture of electrons and ions is derived by an extension of Natanson's theory of charging of small dust particles (Natanson 1960), by taking plausible values for their size and height distribution.

## 2. Direct Determination of the "Effective Recombination Coefficient"

2.1 The multiple frequency cosmic noise absorption data at College during the polar cap event (PCE) in July 1961 were used to derive the $N_e(h)$ profiles (Fig. 2) in the region between 40-90 km. For a full discussion of the profile-derivation technique, reference may be made to Parthasarathy et al (1963); Serafimov and Nestorov (1963); Lerfald et al (1964); Parthasarathy and Berkey (1965). Following the last paper, an electron collision frequency model which takes into account the seasonal variation of atmospheric density was used in conjunction with the Sen-Wyller magneto-ionic equation.

Since the early attempts (Parthasarathy et al, 1963) at profile derivation by means of the multiple-frequency absorption data, several improvements have been made in the exact details of derivation. It has been found that in correcting for the finite beam width of the antenna to obtain the "line integral" of absorption, due cognizance should be made of the fact that the angle of propagation with respect to the magnetic field of the arriving ray is a function of azimuth and zenith angles. It was, however, found that the reduced "line integral" of absorption is not sensitive to the details of the electron density profile in the absorbing region. Even in the case of the 5 Mc/s (ordinary, or extraordinary mode) where the specific absorption coefficient significantly varies with the propagation angle, no more than two

percent differences arose in the reduced "line integral" of absorption when every possible sort of profiles (including thin stratums of electron density) were assumed in the 50 to 100 km region. Further, in most instances the reduced absorption could be fitted in the 5 to 50 Mc/s range by a power law relation, in which the exponent could be specified within an error of $\pm$ 0.1. The derived exponent is not sensibly dependent upon the requirement of strict uniformity of ionization within the antenna beamwidth (of $\pm$ 35 degrees to half-power response) at any altitude. For example, a non-uniformity by a factor of two, makes a difference of only 0.1 to the exponent, and hence only minor difference to the shape of the derived electron density profile. In deriving the electron density profile, best-fitting the observed line integral of abosrption in the eight observing frequencies of $5^-$, $5^+$, $10^-$, $10^+$, $20^-$, $20^+$, 30 and 50 Mc/s, (where - and + sign refer to the extraordinary and ordinary modes respectively) considerably stabler profiles could be derived, and the difference $(\Delta A)_n$ between the profile-derived absorption and the observed absorption at any frequency $f_n$, could be made less if the coefficients of the profile polynomial were sought by the criterion that $\Sigma f_n (\Delta A)_n^2$ be a minimum. The weighting factor $f_n$ was chosen because the experimental error in the absorption datum varied inversely as the square root of the frequency, being $\lesssim$ 0.1 db at 50 Mc/s. G. M. Lerfald of the CRPL (private communication) has independently investigated the above aspects to the profile-derivation and his conclusions are similar.

2.2 Figure 1 shows the reduced absorption versus the frequency during three instances of the PCE of the 20th July, 1961. The corresponding electron density profiles shown in Figure 2 were derived so as to be compatible not only with the data on the four frequencies ($10^-$, $10^+$, 30 and 50 Mc/s) in operation

at that time, but also of the data at $5^-$, $5^+$, $20^-$ and $20^+$ Mc/s as read in the best-fitting lines in Figure 1. The differences, at any of these eight frequencies, between the absorption data in Figure 1 and the absorptions computed from the profiles in Figure 2, were less than two percent. A set of alternate profiles was also derived with a sharp cut-off at a level as high as 40 km, equally satisfactory at these eight frequencies, and coinciding (within 20 percent) with the set in Figure 2 in the 55 to 75 kilometer region; however, the two sets differed almost by a factor of two in the 50 km level, and by a factor of about 1.5 in the 90 km level. The alternate set was discarded only because the absorption computed from it at 100 Mc/s differed drastically from the extrapolated values in Figure 1. On the other hand, when the cut-off level was lowered to 20 km, the resulting set of profiles coincided with the set in Figure 2 within a tolerance of 10 percent in the 55 to 90 km region, but differing by 25 percent at the 50 km level. Based only on these considerations, it can therefore be surmised that the profiles in Figure 2 are valid with an uncertainty of 50 percent at the 85 km level, of 25 percent in the 70 and 60 km levels, and of 50 percent at the 50 km level.

2.3 The instances shown in Figure 1 were chosen during the PCE because, (a) instantaneous proton flux data were available at these instances (Pieper et al 1962) from the Injun I; (b) the absorption levels could be accurately scaled, reduced and fitted by a power law; and (c) the Injun I data showed that the cut-off energy for the geomagnetic latitude of College (64.8°) were as low as about 1.5 Mev at these times.

Pieper et al (1962) have expressed the particle flux obtained from the counters responding to $E > 1.5$ Mev and $E > 40$ Mev by means of a power law $N(>E) \alpha E^{-(x-1)}$. These instances in Figure 1 were characterized by a relatively

hard spectrum, with x of about 2.5. Dr. G. C. Reid of the CRPL has supplied us his model tabulation of ionization rates for the altitudes in the 40 to 90 km region. From Figure 3 which was drawn from his tabulation it can be seen that, given a flux above 1.5 Mev, characterized by a spectrum with (x-1) = 1.5, the ionization rate in the altitudes below the 75 km level does not change when the protons of energy less than 5 Mev were prevented from entering the latitude of College; progressively serious changes happen in the ionization rate at the higher altitudes. While it can be readily seen from Injun I data (Pieper et al, 1962) that during 1921 and 2258 UT, the College cut-off was as low as 1.5 Mev, an uncertainty exists regarding the cut-off during 1541 UT, when the cut-off could have been somewhat higher than 1.5 Mev. Using the proton flux data, the ionization rates at these instances are calculated and are shown in Figure 2. The portion of the curve at 1541 UT, above 75 km may have been overestimated by a factor of two because of the uncertainty in the cut-off. The overall errors in the rates elsewhere may amount to about 20 percent (Reid, private communication).

From Figure 2 the effective recombination coefficient, defined by $q = \alpha_{eff} N_e^2$ was calculated and the mean value of the three instances is shown in Figure 4 for the several altitudes.

2.4 We shall now outline the limitations to the derived $\alpha_{eff}$ in Figure 4. The uncertainty in the coefficient arises from the primary particle data used in the calculation of the ion-pair production rates, and from the derived $N_e(h)$ profiles.

An examination of the several factors that may contribute to the uncertainty in the proton flux and spectrum reveals that the flux and the exponent defining the power-law spectrum may be accurate only within $\pm$ 25 and $\pm$ 10 percent respectively. Based on several balloon-observed data for particles above

100 Mev, Freier and Webber (1963) have presented a case for an exponential rigidity spectrum. This spectrum avoids the obvious mathematical difficulty of the power-law near zero energies, and is able to account approximately for the particles of a few tens of Mev which only the satellites and rockets can measure. It is also well-known that in any limited range of energies (say, less than two orders of magnitude) data uncertainties do not enable a choice between a power-law and an exponential-law fit. We do not, however, consider that an exponential spectrum, best fitting the balloon-observed particles ($E \gtrsim 100$ Mev) could account, with the necessary accuracy, for the particles in the range of 1.5 to 60 Mev which almost wholly control the ionization rate in the altitudes between 40 and 90 kms. For example, from Table 2 of Freier and Webber (1963), the exponential spectrum fitting the balloon-observed, higher energy data gives a flux above 1.5 Mev as 66 particles ($cm^{-2}sec^{-1}ster^{-1}$) at 0200 UT on the 21st of July 1961, in contrast with the flux, measured by the satellite, of about 300 (Fig. 11 of Pieper et al). The use of such an exponential spectrum would therefore underestimate the $\alpha_{eff}$ by a factor of about 5 at the higher altitudes. To summarize: (a) the data from the several satellite borne instruments (published and unpublished) available to date indicate that in the limited energy region of a few Mev to 60 Mev a power law fit is as acceptable as an exponential law fit; (b) the extrapolation of such a law to higher energies (> 60 Mev) will significantly overestimate the flux of higher energy particles; however, such over-estimates lead to only a few percent error in the ion production rates in the 50-90 km region; (c) on the other hand, an exponential spectrum fitting the higher energy particles and extrapolated to the lower energy particles, will lead to unacceptable errors in the ion production rates.

In principle, the greater source of error to Figure 4 arises from the limitations to the derived $N_e(h)$ profiles. These have been discussed in the several multiple-frequency publications referred to in section 2.1. Intrinsic to the profiles derived from the absorption data from a finite number of radio frequencies is the progressively large uncertainty at the altitudes which had not contributed a significant share to the total absorption in any of the frequencies used. For a detailed discussion of this point, see section 2.2.

As pointed out by Webber and Freier (1963), the presence of Alpha-particles in the satellite-measured flux may give rise to a higher ion-pair production rates at the altitudes above about 50 km. The Alpha-particle content is known to differ widely from event to event, but is unlikely to be greater than about 10 percent. The content is unknown at the times shown in Figure 1, and the ionization rate was calculated by assuming all the particles as protons. If a few percent of the flux were assumed to be Alpha-particles, the resulting q and, hence, the $\alpha_{eff}$ would be somewhat <u>higher</u> than those plotted in Figure 4. More reliable and greater volume of observational data on Alpha-particles (than are currently available) would be needed before taking serious cognizance of them in the D-region studies. A source of <u>over-estimation</u> of $\alpha_{eff}$ may be in the uncertainty of the actual flux that should have been used in the calculation of q. The flux measured by Injun I at $\simeq$ 1000 km was assumed to have arrived isotropically towards the station. In the absence of any reliable information regarding the pitch angle function, the possibility of a small fraction of them mirroring from altitudes between the 100 and the 1000 km levels was excluded. The resulting $\alpha_{eff}$ (Fig. 4) could therefore have been slightly overestimated on this account.

Including all the possible sources of error, it would seem that the derived $\alpha_{eff}$ in the region between 50 and 80 km may be accurate to well within $\pm$ 50 percent.

## 3. Steady State Distribution of Electrons and Ions

3.1 The several physical processes leading to the equilibrium distribution of charge density are believed to be the attachment of electrons to neutral particles, recombination of positive and negative ions, electron-positive ion recombination, collisional detachment and photodetachment of negative ions. To these we add the attachment of electrons and positive ions to the dust particles. The effect of the collisional detachment is now believed to be small compared with the other processes and we neglect the collisional detachment. For the rate of change of the charged particle densities we can write the differential equations as follows:

$$\frac{dN^+}{dt} = q - \alpha_i N^+ N^- - \alpha_d N^+ N_e - D^+ N^+ \qquad (1)$$

$$\frac{dN^-}{dt} = AN_e - \alpha_i N^+ N^- - P N^- - D^- N^- \qquad (2)$$

$$D^+ N^+ = D_e N_e + D^- N^- \qquad (3)$$

where $N_e$, $N^+$ and $N^-$ are the electron, positive ion and negative ion number densities, q is the ionization rate, $\alpha_i$ is the ion-ion recombination coefficient, $\alpha_d$ is the dissociative recombination coefficient, A is the electron attachment coefficient to the neutral molecules and P is the photo detachment coefficient. $D_e$, $D^+$ and $D^-$ are the rate coefficients of attachment to the dust particles for electrons, positive ions and negative ions respectively. For the steady state, the number of positive ions captured per second by the

dust particles must be equal to the number of electrons and negative ions captured. The equation (3) is simply a statement of this fact.

For the equilibrium conditions we have,

$$\frac{dN^+}{dt} = \frac{dN^-}{dt} = \frac{dN_e}{dt} = 0$$

(Note, the collisional detachment term could be absorbed by P, day or night.) Hence from equations (1), (2) and (3) we get

$$q = [\alpha_d (\eta + \lambda\gamma) + \{D_e + \lambda D^- + \alpha_i (\eta + \lambda\gamma)N^-\} \frac{1}{N_e} ] N_e^2 \qquad (4)$$

where $$\eta = \frac{D_e}{D^+}$$

$$\gamma = \frac{D^-}{D^+}$$

$$\lambda = \frac{N^-}{N_e}$$

Using the expression $q = \alpha_{eff} N_e^2$ we have

$$\alpha_{eff} = \alpha_d (\eta + \gamma\lambda) + [D_e + \lambda D^- + \alpha_i (\eta + \gamma\lambda)N^-] \frac{1}{N_e}$$

$$= (\eta + \gamma\lambda) (\alpha_d + \lambda\alpha_i) + \frac{D_e + \lambda D^-}{N_e} \qquad (5)$$

3.2 It is pertinent to compare this expression with the one obtained without taking the dust particles into consideration. As shown in section 4.4, the coefficients $D_e$, $D^+$ and $D^-$ each tend to zero, while for $\lambda \lesssim 250$ the ratio $\eta$

tends to $(1+\lambda)$ and $\gamma\lambda$ is relatively negligible, as the dust population goes to zero. Therefore, in the limit of zero dust concentration, we get

$$\alpha_{eff} = (1 + \lambda)\ (\alpha_d + \lambda\alpha_i) \tag{6}$$

which is the usual expression for $\alpha_{eff}$ derived by ignoring the dust particles.

## 4. Determination of the Rate Coefficients $D_e$, $D^+$ and $D^-$

4.1 The presence of dust particles in an ionized gas modifies the electron and ion concentration owing to the capture of these by the dust particles. The particles in the lower ionosphere are mostly of meteoric origin and have a very high dielectric constant. At the altitudes under consideration thermionic emission from these particles is negligible and, in the steady state, the dust will be negatively charged (Shklovskii, 1958). Solar illumination is also believed to be ineffective in detaching the charges from the dust. The problem then is to determine the rate of capture of electrons and ions by these negatively charged dust particles.

4.2 The theory of charging of aerosols by capture of ions has been worked out in detail by Natanson (1960). For determining the capture rate of the ions we adapt his treatment to cover the conditions in the lower ionosphere. The mass of the dust particle is much larger than the ion mass so that the dust particle can be taken to be stationary during the encounter with the ions of thermal velocity. Also, the ions are assumed to be singly charged. For a positive ion, the force of interaction with the dust consists of the Coulomb force and the image force, both of which can be derived from the potential given by

$$\phi(r) = -\frac{Z\epsilon^2}{r} - \frac{\epsilon^2 a^3}{2r^2 (r^2 - a^2)} \tag{7}$$

where Z is the number of elementary changes on the dust particle; $\varepsilon$ is elementary charge [esu]; a is radius of the dust.

In the above expression we have assumed the dust to be perfectly conducting. For a substance of dielectric constant $\kappa$ the image potential term is multiplied by a factor $(\kappa + 1)/(\kappa + 2)$. For dust particles of meteoric origin, their high dielectric constant makes this factor very nearly unity. Due to the presence of the attractive potential, the cross section of the dust particle for positive ion capture is larger than its geometrical cross section.

Natanson's expression for the rate of capture of positive ions by the negatively charged dust reduces to simple forms in the two extreme cases defined by

$$\frac{kTl_i}{Z\varepsilon^2} \gg 1; \text{ and } \frac{kTl_i}{Z\varepsilon^2} \ll 1.$$

where $l_i$ = ion mean free path. Thus, when $\frac{kTl_i}{Z\varepsilon^2} \gg 1$, the rate of capture by the dust,

$$n^+ = 3\pi a \rho C_i N^+ \left[1 + \frac{16}{8l} \frac{l_i}{a} \left( \frac{Z\varepsilon^2}{kTl_i} \right)^2 \right] \tag{8}$$

where $\rho = \frac{Z\varepsilon^2}{3\kappa T}$, $C_i$ = mean thermal velocity of the ions, and $N^+$ is their number density. For the conditions in the lower ionosphere, this expression reduces to

$$n^+ \approx 3\pi a \rho C_i N^+ \approx \pi C_i N^+ \cdot \frac{\varepsilon^2}{kT} aZ \tag{8a}$$

If N(a)da is the number density of the dust particles in the radius range da, the total rate of capture of positive ions per unit volume is simply $\int_0^\infty n^+ N(a)da$. Thus, we have

$$D^+N^+ = \int_o^\infty n^+ N(a)da$$

$$= \pi C_i N^+ \frac{\varepsilon^2}{kT} \int_o^\infty N(a).a.Z.da. \qquad (9)$$

and,

$$D^+ = \pi C_i \frac{\varepsilon^2}{kT} \int_o^\infty N(a).a.Z.da.$$

4.3 Capture of electrons and negative ions

In the case of electrons and negative ions the coulomb potential is repulsive while the image potential is attractive and the total potential is given by

$$\phi(r) = + \frac{Z\varepsilon^2}{r} - \frac{\varepsilon^2 a^2}{2r^2(r^2 - a^2)} \qquad (10)$$

It is no longer possible to neglect the image force which now plays an important role. At large distance from the particle, the force on the electron or negative ion is completely determined by the Coulomb force. As the electron approaches the particle, the image force increases and at a distance $r_o$ from the center of the dust particle, the force becomes attractive and increases rapidly as the distance from the dust surface decreases. Thus the situation is schematically shown in Figure 5. All electrons which are incident on the sphere $r_o$ will thus be captured by the dust particle.

Since the mean free path of the electrons is very large compared to the distances involved, the number of electrons reaching the sphere $r_o$ is approximately given by (Natanson 1960)

$$n_e \approx \pi r_o^2 C_e N_e \exp\left[\frac{-\phi(r_o)}{kT}\right] \qquad (11)$$

where $C_e$ is the mean thermal velocity of the electrons and $N_e$ is their number density.

Qualitatively one can view this problem as the passage of electrons through a potential barrier. The resultant potential for $r \geq r_1$ (Figure 5) is equivalent to a potential barrier with maximum at $r = r_o$. If the energy of the electrons exceeds the maximum of the barrier almost all the incident electrons will reach the capture sphere. If the electron energy is less, the number of the electrons reaching the capture sphere will be determined by the transmission coefficient of the barrier.

The distance $r_o$ is determined by the number Z, and is always greater than a.

Putting $r_o = ga$ we have

$$\phi(r_o) = \frac{Z\varepsilon^2}{ga} \left[1 - \frac{1}{2g(g^2 - 1)Z}\right] \tag{11a}$$

where $1 < g \leq 1.62$ (Natanson 1960). For example, with $Z = 1$, $r_o = 1.62a$ while for $Z = 10$, $r_o = 1.18a$. Thus, for moderate values of Z, the second term on the right hand side of Eq. (11a) is negligible and from (11) we get

$$n_e = \pi g^2 a^2 C_e N_e \exp\left[-\frac{Z\varepsilon^2}{gakT}\right] \tag{12}$$

The total rate of capture by all dust particles is $\int_o^\infty n_e . N(a) . da =$

$$\pi g^2 C_e N_e \int_o^\infty N(a) a^2 \exp\left[-\frac{Z\varepsilon^2}{gakT}\right] da$$

$$D_e = \pi g^2 C_e \int_o^\infty N(a) \cdot a^2 \exp\left[-\frac{Z\varepsilon^2}{gakT}\right] da.$$

It is shown in equation (16.a) that Z/ga is independent of a. Hence,

$$D_e = \pi g^2 C_e \exp\left[-\frac{Z\epsilon^2}{gakT}\right] \int_0^\infty N(a) \cdot a^2 \cdot da \qquad (13)$$

The expression for the capture of negative ions can be derived in an analogous manner and we have

$$n^- = \pi g^2 N^- C_i \cdot \exp\left[-\frac{Z\epsilon^2}{gakT}\right] \qquad (14)$$

$$D^- \simeq \pi g^2 C_i \int_0^\infty N(a)\, a^2 \exp\left[-\frac{Z\epsilon^2}{gakT}\right] da.$$

and, because of equation (16a),

$$D^- = \pi g^2 C_i \exp\left[-\frac{Z\epsilon^2}{gakT}\right] \int_0^\infty N(a) a^2 da \qquad (14a)$$

4.4 Now, the number of positive ions captured by a dust particle increases with the number Z, while the number of electrons and negative ions captured decreases as Z increases. In the stationary state, therefore, Z must be such that the number of positive ions captured is the same as the number of electrons and negative ions captured by each dust. Using the expressions 8a, 12 and 14 for the capture rates,

$$C_e N_e \left(1 + \lambda \frac{C_i}{C_e}\right) \exp\left[-\frac{Z\epsilon^2}{gakT}\right] = \frac{3\rho}{ag^2} C_i N^+ = \frac{Z\epsilon^2}{g^2 akT} C_i N^+ \qquad (15)$$

which gives $Z/ga = \frac{kT}{\epsilon^2} \log_e \left[g^2 \frac{akT}{Z\epsilon^2} \left(\frac{C_e}{C_i} + \lambda\right) \frac{Ne}{N^+}\right]$ (16)

Equation (16) was solved numerically (Fig. 6) and a close approximation (within 10%) for the lower ionosphere ($\lambda << 250$) could be fitted as,

$$\frac{z}{ga} = 9{\cdot}2 \times 10^4 \log_e \left[5 \times 10^3 \, g \frac{Ne}{N^+}\right] \tag{16a}$$

which is independent of the dust radius. For $\eta$ and $\gamma$ then we have,

$$\eta = \frac{g^2 akT}{Z\varepsilon^2} \cdot \frac{C_e}{C_i} \exp\left[-\frac{Z\varepsilon^2}{gakT}\right] \tag{17}$$

$$\gamma = \frac{1}{235}\eta$$

However, the second term in equation (5), i.e. $\dfrac{D_e + \lambda D^-}{N_e}$

contains the radius and the number density of dust explicitly. Noting that $D^-$ is $\frac{1}{235} D_e$, this additive term is very nearly equal to

$$\frac{D_e}{N_e} = \frac{\pi g^2 C_e}{N_e} \exp\left[-\frac{Z\varepsilon^2}{gakT}\right] \int_o^\infty N(a)\, a^2 .da.$$

Expression (17) is not amenable for examining the value of $\eta$ and $\gamma$ in the limiting case of the dust concentration going to zero. It does not depend explicitly upon the number density of dust, nor does it even depend upon the radius a, because Z/a is almost independent of a. (Strictly, however, g has a slight dependence on Z and a, separately (see sections 4.3 and 4.6); and $\lambda$ in equation (16) (which controls equation (17)) must have a degree of dependence on the number density of dust. Such dependences, nevertheless, did not affect the stability of equation (17), because $Z/ga \sim \frac{kT}{\varepsilon^2} = 1.5 \times 10^5$.)

Hence, we consider the requirement that the rate of capture of electrons and negative ions by all the dust equals the rate of capture of the positive ions, i.e., eq. 3.

$$D_e N_e + D^- N^- = D^+ N^+ .$$

Hence,

$$\eta + \gamma\lambda = \frac{N^+}{N_e} = \eta\left(1 + \frac{\lambda}{235}\right) =$$

$$= 1 + \lambda + \int_0^\infty \frac{N(a)\, Z.da}{N_e} \quad \text{(because of charge neutrality)}$$

Then, for $\lambda << 250$,

$\eta \to 1 + \lambda$, and $\gamma\lambda \to 0$, as the dust population tends to zero. Further, $D_e$, $D^+$ and $D^-$ also tend to zero; hence, $\alpha_{eff} = (\alpha_d + \lambda\alpha_i)(1 + \lambda)$.

4.5 The concentration of the dust particles has been the subject of several recent investigations, by means of twilight and rocket observations. From twilight observations, Divari (1964) has shown that the height and size distribution of the dust particles in the lower ionosphere may be expressed as

$$N(h) = 4.8 \times 10^{10} \times h^{-7.2} \ (cm^{-3}) (40 < h < 135 \text{ km}) \tag{18}$$

$$N(a).da = F.a^{-3}.da \ (a > 5 \times 10^{-6} \text{ cm})$$
$$= 8000F \ (a < 5 \times 10^{-6} \text{ cm}) \tag{19}$$

where $F \approx 1.3 \times 10^{-7}$

Divari also points out that for the 80 km level his result is consistent with the rocket observations of Mikirov (1962), but is about two orders of magnitude larger than the values inferred by Volz and Goody (1962) from

twilight observations. Recent rocket observations at 80 km over Sweden by Hemenway et al. (1964) have indicated a size distribution somewhat steeper than Divari's distribution for dust radius > $5 \times 10^{-6}$ cm. We approximate their distribution by the expression

$$N(a)\, da \approx Ka^{-4}\, da \quad (4 \times 10^{-6} < a < 10^{-4} \text{ cm}) \qquad (20)$$

$$\approx 0, \text{ elsewhere.}$$

By combining this size distribution (eq. 20) and the electron attachment rate $D_e$, it is readily seen that the effectiveness of the dust is almost wholly restricted to the particles in the limited radius range of $5 \times 10^{-6}$ to $5 \times 10^{-5}$ cm. While the height dependence of dust concentration shown in equation (18) may be a reasonably valid one, the absolute concentration at any particular altitude, say 80 km, does not appear to be firmly established. Hemenway et al.'s rocket data indicates that the concentration at 80 km is variable in the range of $10^{-3}$ to 1 ($cm^{-3}$).

4.6 To calculate the $\alpha_{eff}$ through equation (5), one then needs to obtain the values of $\lambda$, $\eta$ and $D_e$ at any altitude corresponding to a given value of $N_e$. $\lambda(h)$ has been derived in a number of review papers which also discuss the several molecular processes contributing to $\lambda$. Webber (1962), for example, has given $\lambda(h)$ for the sunlit ionosphere, as well as $\lambda(N_e,h)$ for the dark ionosphere. Because of the large rate of photodetachment compared with the mutual neutralization process, $\lambda$ is not dependent upon $N_e$ during sunlit condition. To claculate $\eta$ and $D_e$, from equations (17) and (13), we note that we need the values of Z/ga which is dependent upon $\frac{N^+}{N_e}$. Using the numerically solved graph (Fig. 6) of Z/ga vs. $\frac{N_e}{N^+}$ from equation (16), we write

$$Z/ga = G\left(\frac{N^+}{N_e}\right)$$

Now $$\frac{N^+}{N_e} = 1 + \lambda + \int_{a_c}^{\infty} \frac{N(a)\ Z.da}{N_e}$$

$$= 1 + \lambda + g\ \left(\frac{Z/ga}{N_e}\right) . \int_{a_c}^{\infty} N(a)\ a.da,$$

because Z/ga is independent of a. With $a_c = 4 \times 10^{-6}$ cm (see, equation (20) the integral may be readily shown to be

$$\int_{a_c}^{\infty} N(a)\ a\ da = 3.1 \times 10^{10}\ K(h).$$

$$\frac{N^+}{N_e} = 1 + \lambda + \frac{3.1 \times 10^{10}\ k(h)\ g}{N_e}\ G\left(\frac{N^+}{N_e}\right) \qquad (21)$$

Taking the total dust population ($a > 4 \times 10^{-6}$) as $1(cm^{-3})$ at 80 km,

$$K(h) = 2 \times 10^{-16} . \left(\frac{80}{h}\right)^{7.2}.$$

As shown by Natanson (1960), g always lies in the range 1.0 to 1.62 for values of Z ranging from infinity to unity. It does not enter sensitively in the expressions, and a check indicated that g = 1.2 is a satisfactory approximation for all heights. For $N_e$ we use the profile in Figure 2. Using, then, Webber's value of $\lambda$, it is a simple matter of using the $G(N^+/N_e)$ graph (i.e., Z/ga vs. $N^+/N_e$ graph) and obtaining the value of Z/ga which satisfied equation (21), and hence, the values of $\eta$ and $D_e$ to be used in equation (5). Table 1 shows the values of $\eta$ and $D_e$ for the three heights of 90, 70 and 50 km, for

different values of $N_e$ at these altitudes. Figure 4 shows the $\alpha_{eff}$ so derived, for the sunlit conditions, along with the observationally derived $\alpha_{eff}$. The computed $\alpha_{eff}$ is in agreement with the observed $\alpha_{eff}$ (within the estimated errors of $\pm$ 50% in the latter) when $\alpha_d$ was assumed as $2.8 \times 10^{-7}$ and $\alpha_i = 1.8 \times 10^{-7}$.

## 5. Discussion of Results

5.1 We shall now examine whether the agreement, within limits of errors, between the observed coefficients and those calculated by taking cognizance of the dust population could be fortuitous.

In a review of the then available literature on ionospheric recombination coefficients, Nicolet and Aikin (1959) have discussed the limitations to the concept of "effective recombination coefficient". They have pointed out that, in general, the efficiency of an ionizing agency varies from one atmospheric constituent to another. Some radiations such as the Lyman-Alpha can ionize only one particular constituent. Furthermore the rate coefficient of recombination of the molecular ions depends on the species. Under these circumstances, the overall effective recombination coefficient is not merely a function of the altitude; at any altitude it should also depend on the detailed nature and flux of the ionizing agency.

In the more recent years, however, it has become evident that the individual dissociative recombination rates of the dominant molecular ions are approximately equal to one another. That is

| | | |
|---|---|---|
| $O_2^+ + e \rightarrow O + O$ | $[1.7 \pm 1.0] \times 10^{-7}$ | (Biondi, 1964) |
| | $[3.8 \pm 1.0] \times 10^{-7}$ | (Kasner et al, 1961] |
| $N_2^+ + e \rightarrow N + N$ | $[2.8 \pm 0.5] \times 10^{-7}$ | (Biondi, 1964) |
| | $[5.9 \pm 1.0] \times 10^{-7}$ | (Kasner et al, 1961) |
| $NO^+ + e \rightarrow N + O$ | $[\approx 5 \times 10^{-7}]$ | (Gunton and Shaw, 1963; see Biondi, 1964) |

Further, in the case of the ionizing agencies such as the high energy protons, electrons and the Bremstrahlung X-rays, the ionization efficiency for each of the constituents $N_2$, $O_2$, and NO is the same (within a few percent). Thus, even in the extreme case of a stratum which is undergoing ionization solely by auroral (or, for that matter, by solar) Lyman-Alpha the resulting $\alpha_{eff}$ for that stratum can differ from the value obtained when it was ionized by electrons, X-rays or protons by a factor $\leq 2.0$.

A difficulty in the application of the observation-derived $\alpha_{eff}$ values (Figure 4) is that they were obtained under conditions of the values of $N_e$ shown in Figure 2. Strictly, then, given the primary ionized spectrum, the derived coefficient will not be of direct use in calculating the steady state electron density at any altitude. We note, however, that the close agreement within the limits of error between the theoretically-derived expression (eq. 5) which includes the role of dust population and the observationally derived $\alpha_{eff}$ implies that the equation is a correct one and that it could be used directly for the purpose of calculating the steady state ionization at any altitude. Calculations indicate that the coefficients in Figure 4 are valid (at 10% accuracy) even when the electron density, at any particular altitude, was different from that in Figure 2 by an order of magnitude. In other words, the $N_e$ dependence of the coefficient is not severe.

5.2 The steady state electron density may be calculated by means of the equation (5) as follows:

$$q = N_e^2 (\alpha_d + \lambda\alpha_i) \eta(1 + \frac{1}{235}) + N_e D_e \qquad (22)$$

Given, then, $\alpha_d$, $\lambda$, $\alpha_i$ and q, at any altitude, the resulting value of equilibrium electron density is simply the value which when used to derive $\eta$ and $D_e$ [see Section 4.6] would satisfy equation (22).

It is readily shown that the $\lambda(h)$ during the daytime is not affected by considering the dust population. For,

$$AN_{eo} = PN_o^- + \alpha_i N_o^+ N_o^- \quad \text{(in the absence of dust)}$$

$$AN_e = PN^- + \alpha_i N^+ N^- + D^- N^- \quad \text{(with the dust)},$$

where A is the attachment coefficient and P is the photodetachment coefficient. For $N_o^+, N^+ \lesssim 10^6$, $(\alpha_i N^+ + D^-)$ is several orders of magnitude smaller than $P(= 0.44)$. Hence,

$$\frac{N_o^-}{N_{eo}} = \frac{N^-}{N_e} = \lambda.$$

Considering, now, the dependence on dust population of the nighttime $\lambda$ values for a particular value of $N_e$ at any stratum

$$\frac{\lambda_o}{\lambda} = \frac{\alpha_i N^+ + D^-}{\alpha_i N_o^+} = \frac{N^+}{N_o^+} \quad \text{(because } D^- \text{ is several orders of magnitude smaller than } \alpha_i N^+\text{)}.$$

But $\frac{N^+}{N_o^+} = \frac{N_e + N^- + C_d}{N_e + N_o^-}$, where $C_d$ is the total number of charges/$cm^3$ on all the dust particles.

Hence,

$$\frac{1 + \lambda + \frac{C_d}{N_e}}{1 + \lambda_o} = \frac{\lambda_o}{\lambda}$$

or,

$$\lambda = \frac{-(1 + \frac{C_d}{N_e}) + \sqrt{(1 + C_d/N_e)^2 + 4(\lambda_o^2 + \lambda_o)}}{2(1 + C_d/N_e)}$$

where,

$$C_d = \int N(a)Z\, da = g(\frac{Z}{ga})(\frac{80}{h})^{7.2}\, 6.2 \times 10^{-6}$$ (See Sections 4.5 and 4.6.)

We note from Figure 8, that $(\frac{Z}{ga})$ ranges, under the possible conditions in the lower ionosphere, from $2 \times 10^5$ to $6 \times 10^5$. Hence, for $N_e \gtrsim 100$, $C_d/N_e << 1$ and

$$\lambda = \frac{-1 + \sqrt{1 + 4(\lambda_o^2 + \lambda_o)}}{2} \approx \lambda_o$$

Hence, we conclude that the presence of dust does not alter seriously the nighttime values of $\lambda$, appropriate to a given value of $N_e$.

These results may also be surmised from simple physical considerations. Because of the negligibly smaller rate of negative ion attachment to dust compared with the rate of electron attachment to dust, every second as many electrons are lost to dust as are the positive ions. Hence, the existence of dust can be considered as merely a loss of ionization rate, with no effect on the value of $\lambda$, day or night.

5.3 The several molecular processes that enter in the calculation of $\lambda$ ($= N^-/N_e$), such as the attachment of electrons to molecules, photodetachment, as well as the dissociative, and ion-ion recombination coefficients have been the subject of considerable interest in the recent past. Excellent reviews of these processes are given by Biondi (1964), Fite (1964) and Branscomb (1964).

These processes have also been examined from the ionospheric standpoint by Whitten and Poppoff (1964) and Reid (1963). The uncertainties that exist in our calculations of $\alpha_{eff}$ (for example, the dust concentration estimates that we have adopted), are such that it is entirely premature to interpret the close agreement with the observed values of $\alpha_{eff}$ to the correctness of the $\lambda$ models used or the values of $\alpha_d$ and $\alpha_i$. We may only infer that the agreement may be suggestive of their approximate validity, and that it is unlikely to be fortuitous. The choice of $\alpha_d = 5.9 \times 10^{-7}$ would lead to a closer agreement at 70 km level, but the uncertainty in the observed coefficient at $\gtrsim$ 80 km does not permit a valid inference of this.

Laboratory measured coefficients are well known to be uncertain in as much as the coefficients emerged as a result of a quite complex set of reactions. Furthermore, the molecular composition as well as their variability with the ionization of the lower ionosphere are again only imperfectly understood. Our calculations, however, indicate that the dust concentration at any altitude is one of the more significant parameters in the region. With repeated and more accurate estimates of the concentration by rocket-borne instruments the problem of effective recombination coefficient is expected to reach a progressively more reliable state. With the charge/mass ratio of the dust several orders of magnitude smaller than of the molecular negative ions and electrons, mobility experiments using Gerdian condensers may be a feasible approach to the investigation of the dust concentration.

Acknowledgement

We are indebted to Prof. K. B. Mather for his encouragement of the investigation. The investigation was supported by the National Aeronautical and Space Administration contract NAS-5-3595, and partly (Section 2) by the Advanced Research Projects Agency contract ARPA 183/61.

TABLE 1.

| | h = 90 km | | | h = 70 km | | | h = 50 km | | | Entry |
|---|---|---|---|---|---|---|---|---|---|---|
| $N_d$ (80) | 0.1 | 1.0 | 10.0 | 0.1 | 1.0 | 10.0 | 0.1 | 1.0 | 10.0 | |
| $N_e$ | | | | | | | | | | |
| $10^1$ | $6.15^5$ | $6.05^5$ | $4.90^5$ | $5.20^5$ | $4.80^5$ | $3.60^5$ | $1.80^5$ | $1.80^5$ | $1.50^5$ | |
| $10^2$ | $6.20^5$ | $6.15^5$ | $6.05^5$ | $5.30^5$ | $5.20^5$ | $4.80^5$ | $1.80^5$ | $1.80^5$ | $1.80^5$ | |
| $10^3$ | $6.20^5$ | $6.20^5$ | $6.15^5$ | $5.30^5$ | $5.30^5$ | $5.20^5$ | $1.80^5$ | $1.80^5$ | $1.80^5$ | Z/ga |
| $10^4$ | $6.20^5$ | $6.20^5$ | $6.20^5$ | $5.30^5$ | $5.30^5$ | $5.30^5$ | $1.80^5$ | $1.80^5$ | $1.80^5$ | |
| $10^5$ | $6.20^5$ | $6.20^5$ | $6.20^5$ | $5.30^5$ | $5.30^5$ | $5.30^5$ | $1.80^5$ | $1.80^5$ | $1.80^5$ | |
| $10^1$ | 1.14 | 1.23 | 3.18 | 2.56 | 3.60 | 10.70 | 64.50 | 64.50 | 103.50 | |
| $10^2$ | 1.09 | 1.14 | 1.23 | 2.32 | 2.56 | 3.60 | 64.50 | 64.50 | 64.50 | |
| $10^3$ | 1.09 | 1.09 | 1.14 | 2.32 | 2.32 | 2.56 | 64.50 | 64.50 | 64.50 | $\eta$ |
| $10^4$ | 1.09 | 1.09 | 1.09 | 2.32 | 2.32 | 2.32 | 64.50 | 64.50 | 64.50 | |
| $10^5$ | 1.09 | 1.09 | 1.09 | 2.32 | 2.32 | 2.32 | 64.50 | 64.50 | 64.50 | |
| $10^1$ | $1.24^{-6}$ | $1.32^{-5}$ | $2.85^{-4}$ | $1.42^{-5}$ | $1.85^{-4}$ | $4.10^{-3}$ | $1.43^{-3}$ | $1.43^{-2}$ | $1.67^{-1}$ | |
| $10^2$ | $1.20^{-6}$ | $1.24^{-5}$ | $1.32^{-4}$ | $1.31^{-5}$ | $1.42^{-4}$ | $1.85^{-3}$ | $1.43^{-3}$ | $1.43^{-2}$ | $1.43^{-1}$ | |
| $10^3$ | $1.20^{-6}$ | $1.20^{-5}$ | $1.24^{-4}$ | $1.31^{-5}$ | $1.31^{-4}$ | $1.42^{-3}$ | $1.43^{-3}$ | $1.43^{-2}$ | $1.43^{-1}$ | $D_e$ |
| $10^4$ | $1.20^{-6}$ | $1.20^{-5}$ | $1.20^{-4}$ | $1.31^{-5}$ | $1.31^{-4}$ | $1.31^{-3}$ | $1.43^{-3}$ | $1.43^{-2}$ | $1.43^{-1}$ | |
| $10^5$ | $1.20^{-6}$ | $1.20^{-5}$ | $1.20^{-4}$ | $1.31^{-5}$ | $1.31^{-4}$ | $1.31^{-3}$ | $1.43^{-3}$ | $1.43^{-2}$ | $1.43^{-1}$ | |

(Any entry $a^{\pm b}$ in the columns 2 - 10, should be read as $a \times 10^{\pm b}$)

Values of Z/ga, $\eta$ and $D_e$ at the altitudes of 90, 70 and 50 km with the choice of electron density $N_e(CM^{-3})$ ranging from $10^1$ to $10^5$. Three choices of dust concentration $N_d$ at the 80 km ($N_d(80)$) were considered, namely, 0.1, 1.0 and 10 ($CM^{-3}$), in conjunction with the height dependence of $h^{-7.2}$ (see, Section 4.5). Any entry $a^{\pm b}$ in the columns 2-10 should be read as $a \times 10^{\pm b}$.

## References


Adams, G. W. and A. J. Masley, Production rates and electron densities in the lower ionosphere due to solar cosmic rays, J. Atmos. Terr. Phys. 27, 289, 1965.

Bailey, D. K., Abnormal ionization in the lower ionosphere associated with cosmic ray flux enhancements, Proc. I.R.E., 47, 255, 1959.

Belrose, J. S. et al, Physical properties of the polar winter ionosphere obtained from low frequency propagation and partial reflection studies, Radio Sci. J., 68D, 1319, 1964.

Biondi, M. A., Electron ion recombination, Annales De Geophysique, 20, 34, 1964.

Branscomb, L. M., A review of photodetachment and related negative ion processes relevant to aeronomy, Annales De Geophysique, 20, 88, 1964.

Dimick, R. C. and S. L. Soo, Scattering of electrons and ions by dust particles in a gas, Phys. of Fluids, 7, 1638, 1964.

Divari, G., The dust concentration in the upper layers of the earth's atmosphere, Geomagnetism and Aeronomy, IV, 688, 1964.

Fite, W. L., Charge transfer and ion atom interchange collisions above thermal energies, Annales De Geophysique, 20, 47, 1964.

Frier, P. S. and W. R. Webber, Exponential rigidity spectrums for solar flare cosmic rays, J. Geophys. Res., 68, 1605, 1963.

Hemenway, C. L. et al, Sampling of noctilucent cloud particles, Tellus, 16, 84, 1964.

Hemenway, C. L. et al, Electron microscope studies of noctilucent cloud particles, Tellus, 16, 96, 1964.

Lerfald, G. M., C. G. Little and R. Parthasarathy, Study of D-region electron density profiles during auroras, J. Geophys. Res., 69, 2857, 1964.

Kasner, W. K., W. A. Rogers, and M. A. Biondi, Electron-ion recombination coefficients in nitrogen and oxygen, Phys. Rev. Letters, 7, 321, 1961.

McDiarmid, I. B. and E. E. Budzinski, Angular distributions and energy spectra of electrons associated with auroral events, Canad. J. Phys., 42, 2048, 1964.

Mikirov, A. Ye, Aerosol scattering coefficient measurements at 80-100 km, Space research symposium, COSPAR (North Holland Pub. Co.), 155, 1962.

Mitra, A. P., Time and height variation in the daytime processes in the ionosphere, J. Geophys. Res., 64, 733, 1959.

Natanson, G. L., On the theory of charging of amicroscopic aerosol particles as a result of capture of gas ions, Soviet Phys.-Tech. Phys., 4, 538, 1960.

Nicolet, M. and A. C. Aikin, The formation of D-region of the ionosphere, J. Geophys. Res., 65, 1469, 1960.

Parthasarathy, R. and F. T. Berkey, Multiple frequency investigation of radiowave absorption during the dawn breakup phase of aurora, Radio Sci. J., 69D, 415, 1965.

Parthasarathy, R., G. M. Lerfald and G. C. Little, Derivation of electron density profiles in the lower ionosphere using radio absorption measurements at multiple frequencies, J. Geophys. Res., 68, 3581, 1963.

Peiper, G. F. et al, Solar protons and magnetic storm in July 1961, J. Geophys. Res., 67, 4959, 1962.

Reid, G. C., Physical processes in D-region, Reviews of Geophysics, 2, 311, 1963.

Rosen, G., Method for removal of free electrons in a plasma, Phys. of Fluids, 5, 737, 1962.

Serafimov, K. and G. Nestorov, A method of determining the electron density profile in the D-region of the ionosphere, Geomagnetism and Aeronomy, III, 852, 1963.

Shklovskii, I. S., The interplanetary medium and some problems of the physics of the upper atmosphere, Soviet Phys. A. J., 2, 516, 1958.

Volz, F. E. and R. M. Goody, The intensity of the twilight and upper atmospheric dust, J. Atmos. Sci., 19, 351, 1962.

Webber, W. R., Free electrons in the D-region, J. Geophys. Res., 67, 5091, 1962.

Whitten, R. C. and I. G. Poppoff, Ion kinetics in the lower ionosphere, J. Atmos. Sci., 21, 117, 1964.

Whitten, R. C. et al, Effective recombination coefficients in the lower ionosphere, J. Geophys. Res., 70, 1737, 1965.

## Figure Captions

Fig. 1 Reduced, line integral of absorption versus frequency.

Fig. 2 Electron density ($N_e$) and ionization rate (q) profiles during the absorption events shown in Figure 1.

Fig. 3 Ionization rate for the different altitudes versus the low energy cut-off ($E_c$) when the primary spectrum could be specified by $N(>E) = E^{-1.5}$ ($cm^{-2}$ $sec^{-1}$). The primary spectrum is shown in the insert figure.

Fig. 4 The effective recombination coefficient versus altitude: The solid dot at any altitude is the mean $\alpha_{eff}$ during the 3 instances of absorption in Figure 2. The continuous line and dotted lines were calculated by means of equation (5) corresponding to the choices of 80 km dust concentration equals 0.1 ($cm^{-3}$) and 1.0 ($cm^{-3}$) respectively. As an insert is shown the $\lambda(h)$ used in the calculations, after Webber (1962).

Fig. 5 Schematic representation of the interaction potential between the negatively charged dust and an electron or negative ion.

Fig. 6 Numerically solved relation between $Z/ga$ and $\frac{N^+}{N_e}$ obtained from equation (16).

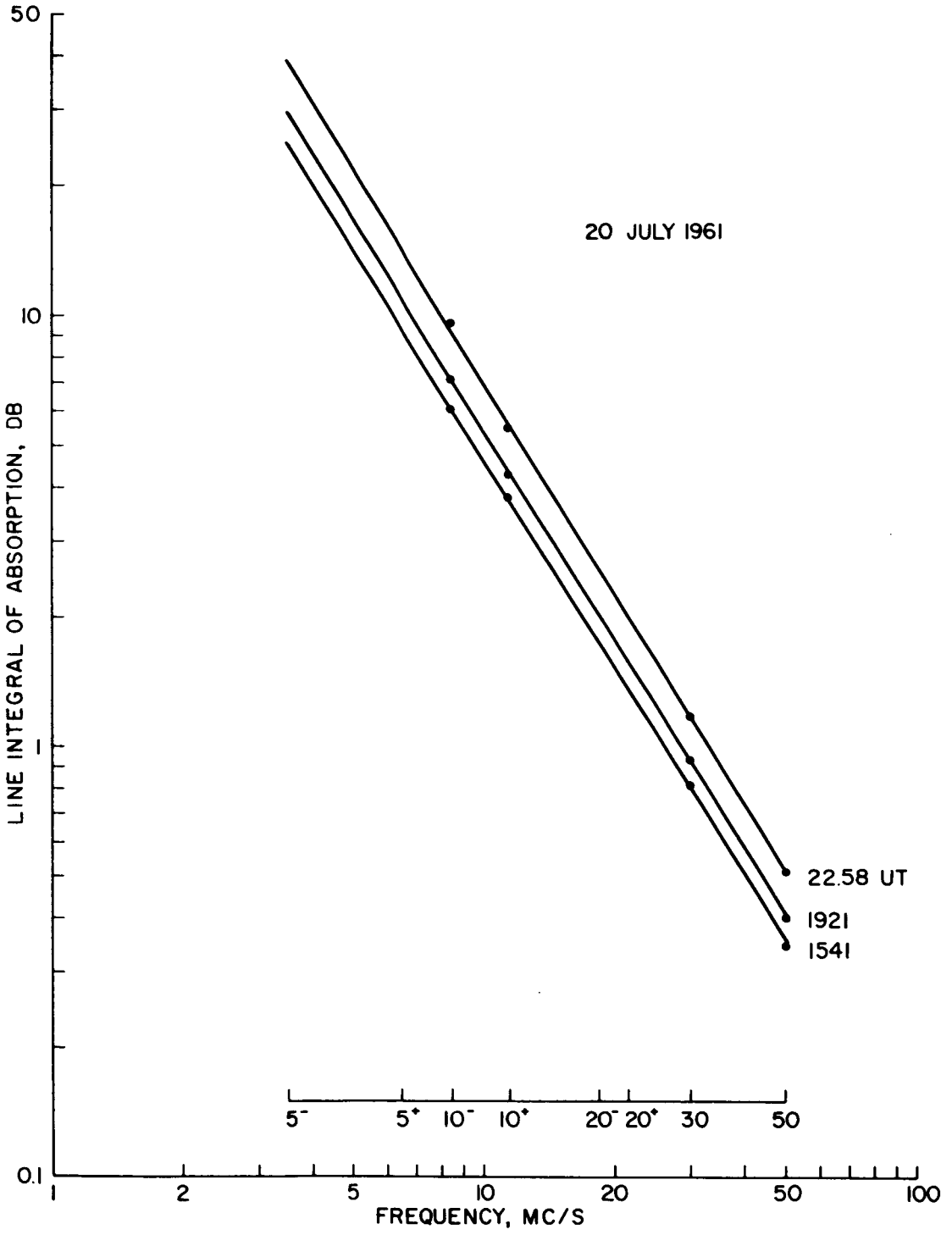


Fig. 1. Reduced, line integral of absorption versus frequency.

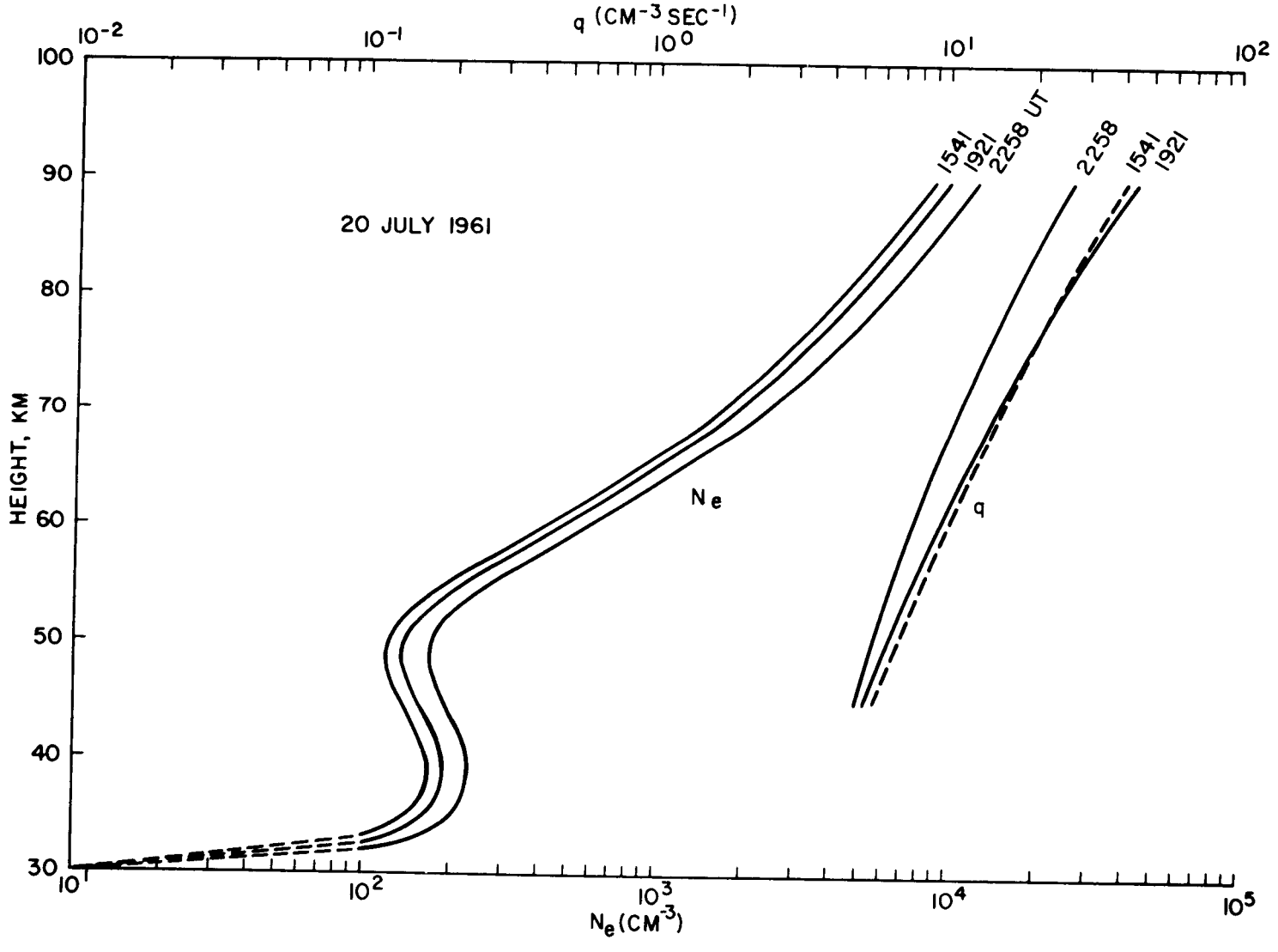


Fig. 2. Electron density ($N_e$) and ionization rate (q) profiles during the absorption events shown in Figure 1.

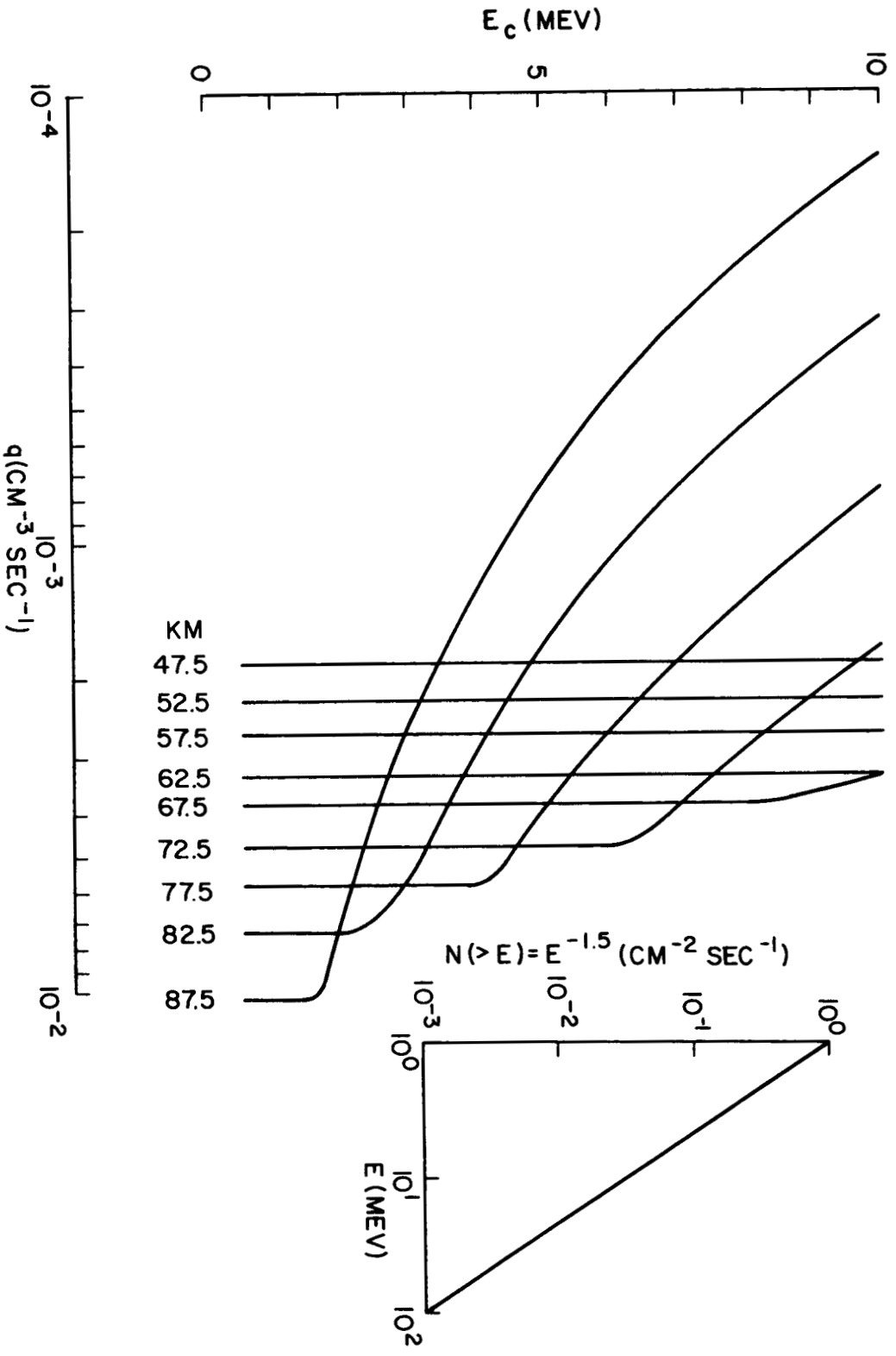


Fig. 3. Ionization rate for the different altitudes versus the low energy cut-off ($E_c$) when the primary spectrum could be specified by $N(>E) = E^{-1.5}$ ($cm^{-2}$ $sec^{-1}$). The primary spectrum is shown in the insert figure.

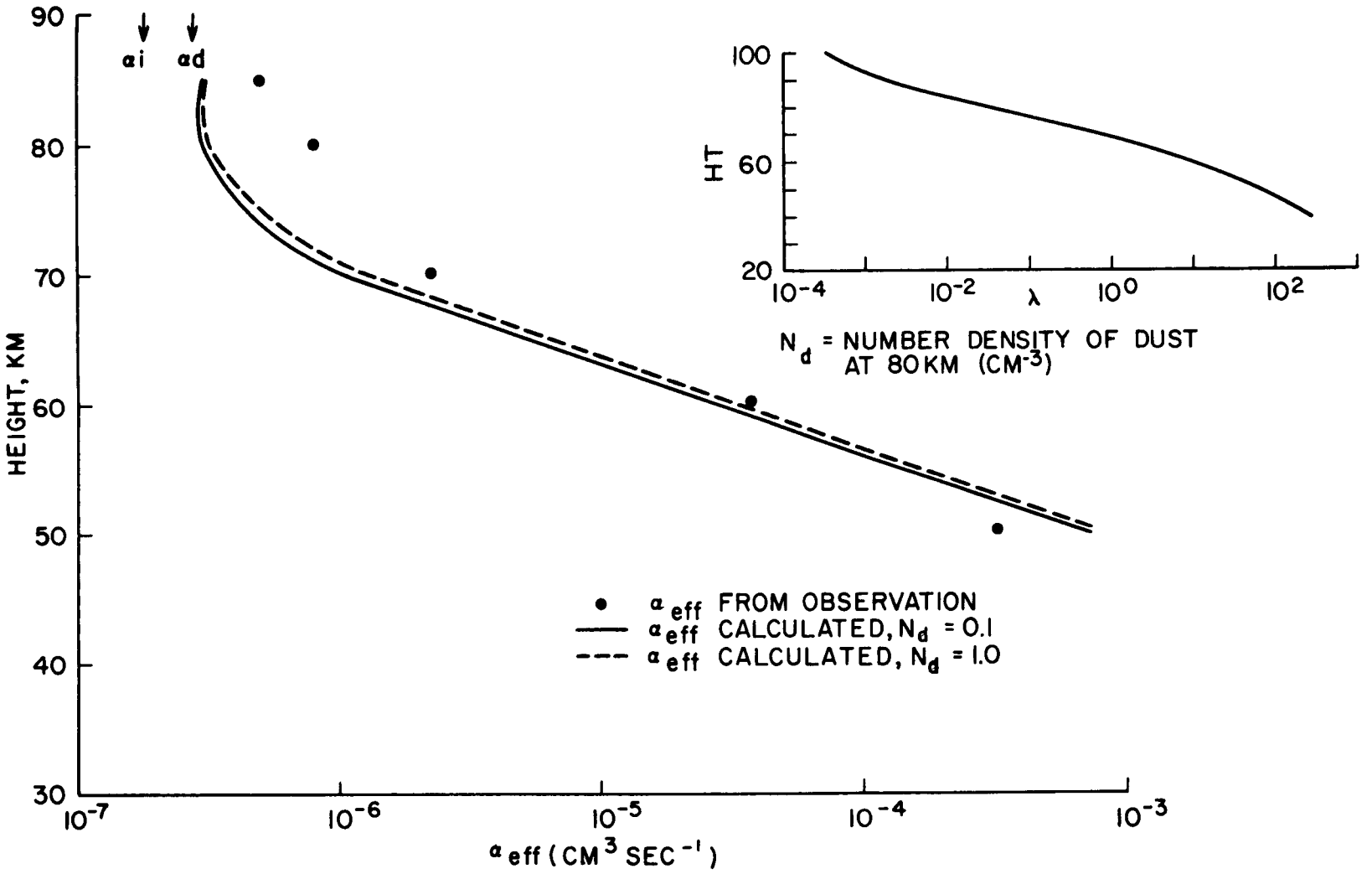


Fig. 4. The effective recombination coefficient versus altitude: The solid dot at any altitude is the mean $\alpha_{eff}$ during the 3 instances of absorption in Figure 2. The continuous line and dotted lines were calculated by means of equation (5) corresponding to the choices of 80 km dust concentration equals 0.1 ($cm^{-3}$) and 1.0 ($cm^{-3}$) respectively. As an insert is shown the $\lambda(h)$ used in the calculations, after Webber (1962).

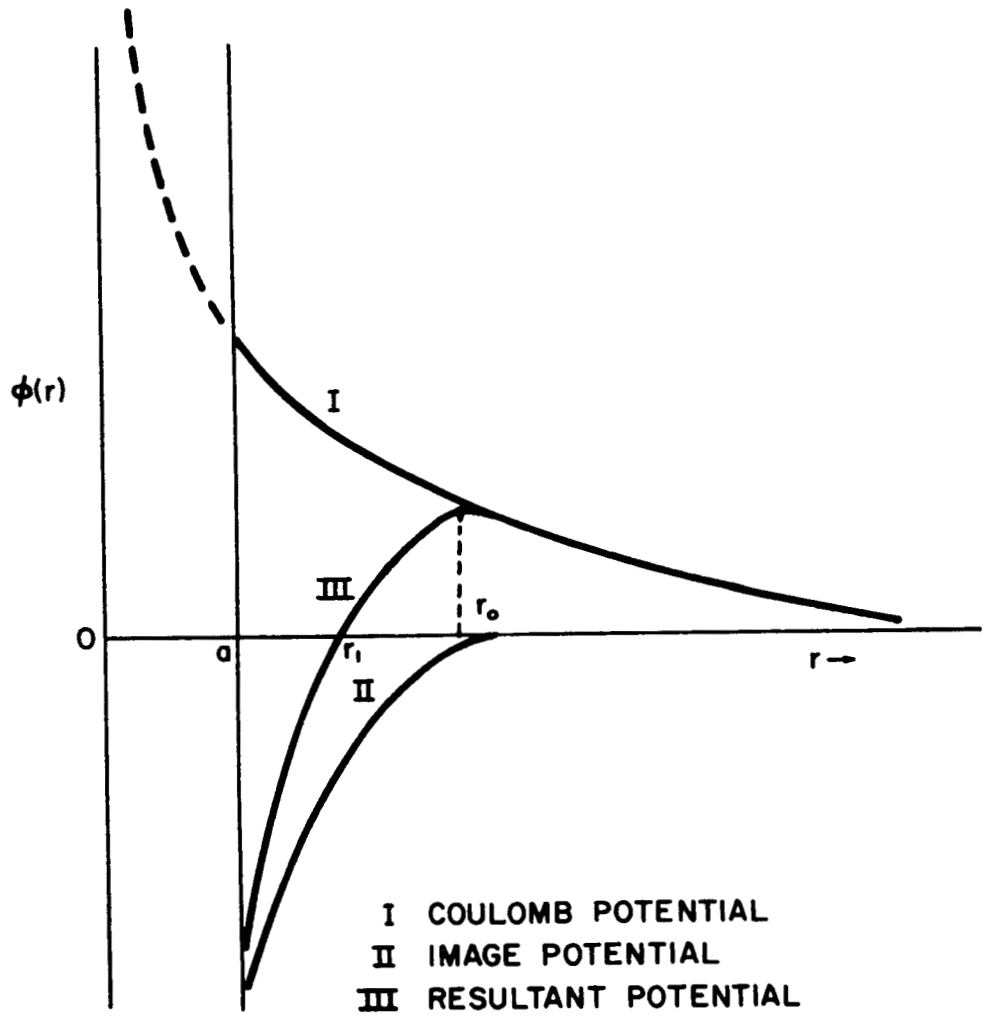


Fig. 5. Schematic representation of the interaction potential between the negatively charged dust and an electron or negative ion.

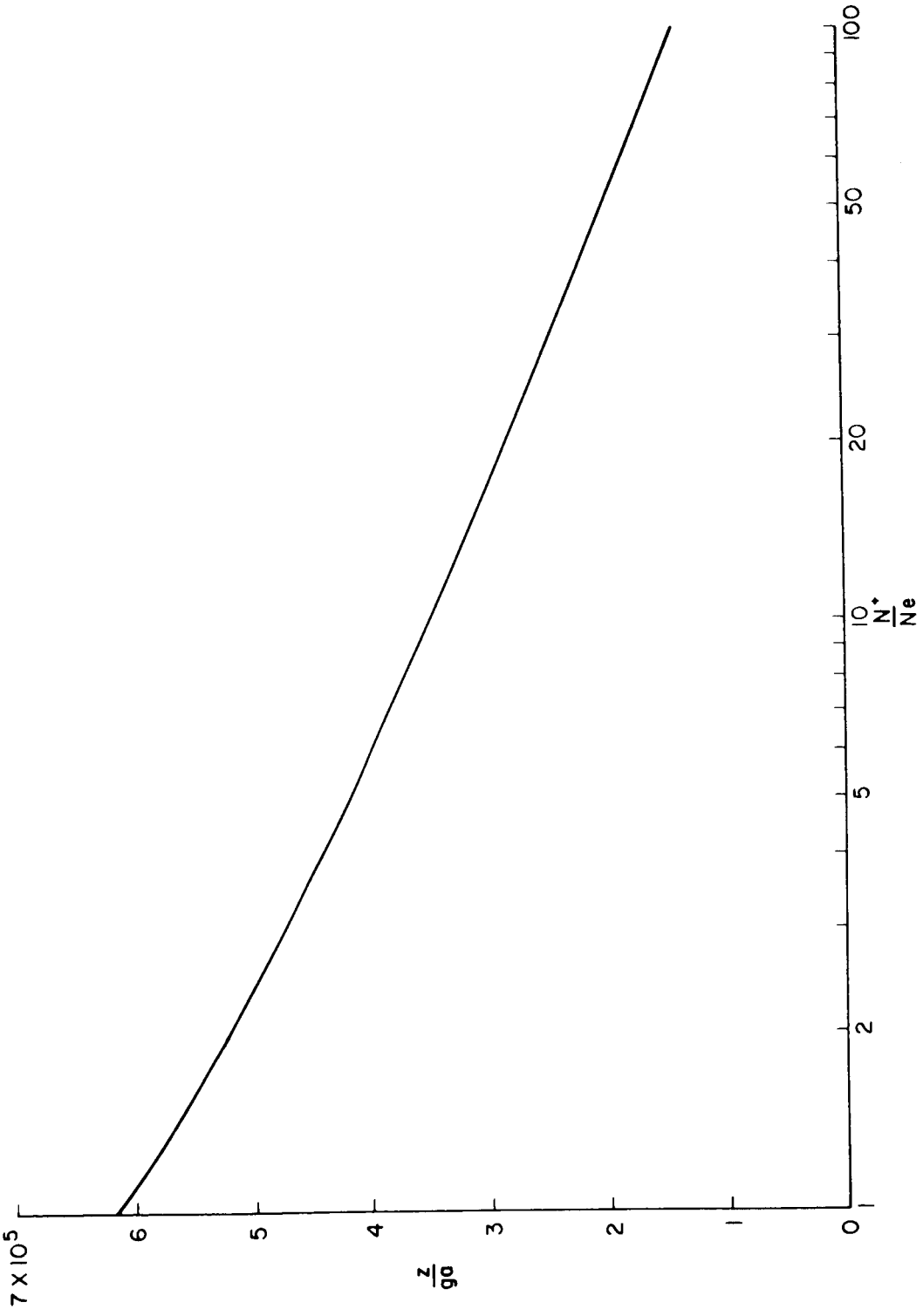


Fig. 6. Numerically solved relation between Z/ga and $\frac{N^+}{N_e}$ obtained from equation (16).